Dynamic Enhancement of Fluctuation Signals at the QCD Phase Transition

Christoph Herold[ab], **Marlene Nahrgang**[*bc], **Igor Mishustin**[bd] **and Marcus Bleicher**[ab],

[a]*Institut für Theoretische Physik, Goethe-Universität, Max-von-Laue-Str. 1, 60438 Frankfurt am Main, Germany*
[b]*Frankfurt Institute for Advanced Studies (FIAS), Ruth-Moufang-Str. 1, 60438 Frankfurt am Main, Germany*
[c]*Department of Physics, Duke University, Durham, North Carolina 27708-0305, USA*
[d]*Kurchatov Institute, National Research Center, 123182 Moscow, Russia*

E-mail: herold@fias.uni-frankfurt.de, marlene.nahrgang@phy.duke.edu, mishustin@fias.uni-frankfurt.de, bleicher@fias.uni-frankfurt.de

We study the impact of nonequilibrium effects on the relevant signals within a chiral fluid dynamics model including explicit propagation of the Polyakov loop. An expanding heat bath of quarks is coupled to the Langevin dynamics of the order parameter fields. The model is able to describe relaxational processes, including critical slowing down and the enhancement of soft modes near the critical point. At the first-order phase transition we observe domain formation and phase coexistence in the sigma and Polyakov loop field leading to a significant amount of clumping in the energy density. This effect gets even more pronounced if we go to systems at finite baryon density. Here the formation of high-density clusters could provide an important observable signal for upcoming experiments at FAIR and NICA. We conclude that improving our understanding of dynamical symmetry breaking is important to give realistic estimates for experimental observables connected to the QCD phase transition.

---

*Speaker.

1. Introduction

Lattice calculations of quantum chromodynamics (QCD) at vanishing baryochemical potential predict a phase transition between hadronic and partonic degrees of freedom, which is an analytic crossover [1, 2, 3]. The question of the nature of the phase transition at finite baryochemical potential μ is a yet unsolved issue. Lots of effort is put into the discovery of a first-order phase transition at large baryochemical potential and a critical point at the end of this phase transition line. Experimentally, this effort is centered on the beam energy scan that is conducted at RHIC where large event-by-event fluctuations are expected at the critical point [4, 5, 6]. Further facilities are built to explore the phase diagram at even higher baryonic densities (FAIR, NICA). From the theoretical side, lattice QCD simulations are constantly improved but the feasibility of calculations at large μ is intrinsically limited by the fermionic sign problem. Effective models are able to reproduce several characteristics of QCD, such as chiral symmetry breaking and restoration. Important features of the gluon dynamics leading to confinement can, however, not be captured in these models, although an effective description via the Polyakov-loop results in statistical confinement at lower temperatures [7, 8, 9, 10, 11, 16, 12, 13, 14, 15]. For the investigation of the QCD phase diagram by heavy-ion collisions dynamical models of the phase transition are needed, because the systems created in heavy-ion collisions differ from thermal systems in the following aspects: They are finite in space and time, inhomogeneous, highly dynamically and the evolution is likely to occur out-of-equilibrium near the critical point and a first-order phase transition.

At the critical point this is due to the phenomenon of critical slowing down, since not only the correlation length diverges but so does the relaxation time. Any system that evolves in a finite time through the critical point will thus necessarily be driven out of equilibrium even if it is equilibrated at a temperature above T_c. From a phenomenological approach including dynamical critical exponents it was found that the correlation grows up to $\xi \sim 1.5 - 2.5$ fm [17]. These nonequilibrium effects will consequently weaken the expected increase of the event-by-event fluctuations at a critical point.

Nonequilibrium effects play, however, an important role at the first-order phase transition in order to observe fluctuation signals in single event studies. When nucleation times are small, one expects spinodal decomposition [18, 19, 20, 21, 22, 23, 24] to dominate the relaxation process leading to an instability of slow modes. In these proceedings we focus on the first-order transition and address the question of how much spinodal instabilities at high baryon densities can facilitate the formation of inhomogeneities and clustering.

2. Nonequilibrium chiral fluid dynamics

Our goal is to combine a description of phase transitions with a realistic modeling of the dynamics of the bulk matter in a heavy-ion collision. For this latter purpose fluid dynamic simulations have proven a very successful tool especially after the discovery of the almost perfect fluid by RHIC. Since the early application of fluid dynamic calculations to high-energy heavy-ion collisions, there has been a lot of improvements. Modern fluid dynamical codes are $3 + 1$d, include viscous corrections, different initial conditions can be included and tested including event-by-event

initial fluctuations [25] and fluid dynamics are used as part of highly developed hybrid models to describe hadronic final interactions [26].

The phase transition is implemented via the Polyakov-loop extended quark meson model. The fermionic part in the presence of the temporal gauge field A_0 is integrated out and treated fluid dynamically by assuming that time scales are much shorter than those which determine the critical fluctuations. The mesonic part, where the sigma field is the order parameter, is propagated explicitly taking into account the interaction with the fluid dynamic part. This setup was derived consistently within the two-particle irreducible (2PI) effective action approach in [27]. This results in a Langevin-type propagation of the sigma field

$$\partial_\mu \partial^\mu \sigma + \frac{\delta U}{\delta \sigma} + g\rho_s + \eta_\sigma \partial_t \sigma = \xi_\sigma \,, \tag{2.1}$$

where U is the classical mesonic potential including a small term of explicit chiral symmetry breaking due to the finite current quark masses, g is the coupling between the fermionic and mesonic fields and ρ_s is the pseudoscalar density. We do not consider fluctuations in the pionic sector. The pion fields are thus assumed to be at their equilibrium expectation value $\langle \vec{\pi} \rangle_{\text{eq}} = 0$. Due to the interaction between the sigma field and the (anti)quarks from the fluid the sigma field is damped by a temperature-dependent damping coefficient η_σ

$$\eta_\sigma = g^2 \frac{d_q}{\pi} \left[1 - 2n_{\text{F}} \left(\frac{m_\sigma}{2} \right) \right] \frac{1}{m_\sigma^2} \left(\frac{m_\sigma^2}{4} - m_q^2 \right)^{3/2} \,. \tag{2.2}$$

With respect to the dissipation-fluctuation theorem the noise field ξ_σ needs to be included on the right hand side of the Langevin-equation (2.1). It is approximated as white noise. Its expectation value vanishes

$$\langle \xi_\sigma(t) \rangle_\xi = 0 \,, \tag{2.3}$$

and the noise correlation is given by

$$\langle \xi_\sigma(t,\vec{x}) \xi_\sigma(t',\vec{x}') \rangle_\xi = \frac{1}{V} \delta(t-t') \delta(\vec{x}-\vec{x}') m_\sigma \eta_\sigma \coth \left(\frac{m_\sigma}{2T} \right) \,. \tag{2.4}$$

In all calculations the equilibrium sigma mass m_σ is used. Below the phase transition, where the sigma mass decreases and the (anti)quarks acquire their constituent mass of around 300 MeV, the leading process that contributes to the damping, the scattering $\sigma \to q\bar{q}$ is kinematically not possible anymore. It is known, however, that there will be an additional damping from $\sigma \to 2\pi$. In this case, we use $\eta_\sigma = 2.2/\text{fm}$, as was approximated in previous studies [28, 29].

Recently we extended the model to include the nonequilibrium dynamics for the Polyakov-loop as well [32, 34]. An analogous derivation of the equation of motion of the Polyakov loop is not possible, we therefore propagate it by a phenomenological relaxation equation, treating ℓ as an effective field [32]

$$\eta_\ell \partial_t \ell T^2 + \frac{\partial V_{\text{eff}}}{\partial \ell} = \xi_\ell \,. \tag{2.5}$$

Here, we assume a parametric value of $\eta_\ell = 5/\text{fm}$. The final, qualitative results are mostly independent of this special choice. Again the stochastic noise is approximated as Gaussian with a zero expectation value and the imposed dissipation-fluctuation theorem to give its variance

$$\langle \xi_\ell(t,\vec{x}) \xi_\ell(t',\vec{x}') \rangle_\xi T^2 = \frac{1}{V} \delta(t-t') \delta(\vec{x}-\vec{x}') 2\eta_\ell T \,. \tag{2.6}$$

The effective potential V_{eff} is described as the sum of the sigma, effective Polyakov loop and mean-field quark-antiquark contribution [32]

$$V_{\text{eff}} = U(\sigma) + \mathscr{U}(\ell, T) + \Omega_{q\bar{q}}(\sigma, \ell, T, \mu) . \tag{2.7}$$

The (anti)quark fluid expands and cools according to energy-momentum and net-baryon number conservation, i. e. the ideal relativistic fluid dynamic equations. In view of the Langevin dynamics of the order parameter the fluid acts as a heat bath. In a heavy-ion collision the system is finite and we thus need to include explicitly the momentum exchange between the sigma field and the fluid. This is done by including a source term to the fluid dynamic equations of energy and momentum conservation

$$\partial_\mu T^{\mu\nu}(t, \vec{x}) = S^\nu(t, \vec{x}) = -(\partial_\mu T_\sigma^{\mu\nu}(t, \vec{x}) + \partial_\mu T_\ell^{\mu\nu}(t, \vec{x})) , \tag{2.8}$$

$$\partial_\mu N^\mu(t, \vec{x}) = 0 . \tag{2.9}$$

This leads to an overall conservation of energy of the coupled system [31, 32]. Since the evolution of the sigma field is manifestly stochastic the source term is stochastic as well, introducing fluctuations in the fluid dynamical fields. This is an important feature as it gives the possibility of studying fluctuations not only in the order parameter fields but also in the thermodynamical quantities like the energy density and the net-baryon density. It is important to note that conventional fluid dynamics only propagates local thermal averages. Recently, the theory of fluid dynamical fluctuations has been extended to applications in heavy-ion collisions [33]. This yields an interesting further approach to investigate fluctuations at the QCD phase transition within fluid dynamical descriptions, but is not an ingredient of our model.

Finally, the system evoles under an equation of state, which depends as well on the local values of the sigma field and the Polyakov loop assuming that the fluid is locally in equilibrium corresponding to the actual value of the order parameter fields

$$p(\sigma, \ell, T, \mu) = -\Omega_{q\bar{q}} , \tag{2.10}$$

$$e(\sigma, \ell, T, \mu) = T\frac{\partial p}{\partial T} + \mu\frac{\partial p}{\partial \mu} - p , \tag{2.11}$$

$$n(\sigma, \ell, T, \mu) = \frac{\partial p}{\partial \mu} . \tag{2.12}$$

For details about the model and first numerical implementations, see [27, 30, 31, 32].

3. Trajectories in the phase diagram

In the following we solve equations (2.1), (2.5), (2.8) and (2.9) numerically for different initial conditions, probing the crossover, critical point and first-order phase transition regime in the (T-μ)-plane. We extract trajectories by averaging the temperature and chemical potential in each time step in a small central volume of $1\,\text{fm}^3$. Results are shown in Fig. 1. We see that the curves follow the behavior of the equilibrium isentropes to bend towards the direction of larger μ when crossing the transition line, cf. [35]. This is connected to the rapid growth of the dynamically generated quark mass at the chiral phase boundary. However, with larger chemical potential, we see that
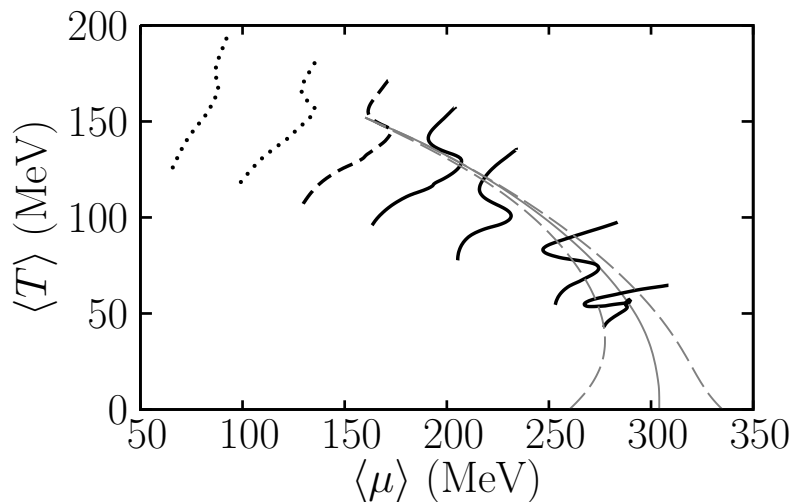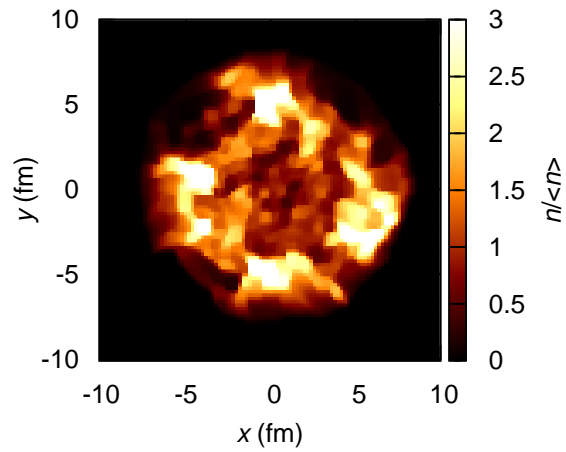
Figure 1: Trajectories of the hydrodynamic simulation in the phase diagram for different initial conditions. Nonequilibrium effects lead to an overshooting of the first-order phase transition. The dashed gray lines denote the spinodal region.

this effect occurs only after the system has left the spinodal region, indicating the formation of a supercooled phase. After the decay of that phase, the system is pushed back into the spinodal region, the extended amount of time here should facilitate the process of spinodal decomposition. We have seen in [32] already for systems at vanishing chemical potential, that this leads to domain formation in the order parameter fields and inhomogeneities in the energy density at a first-order phase transition.
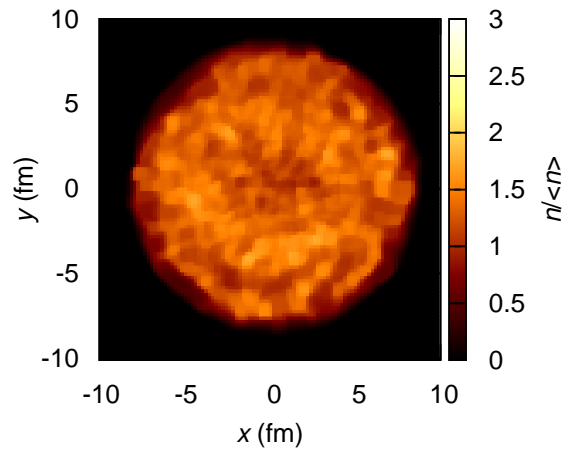
4. Domain formation in net-baryon density

In order to visualize also the domain formation in net-baryon density, we extract the relative net-baryon density $n/\langle n \rangle$ in the transverse $z = 0$ plane. Here $\langle n \rangle$ is the volume averaged net-baryon density over all fluid dynamical cells with $n > 0$. The results are shown in Fig. 2 for an evolution after $t = 9$ fm. We find a large inhomogeneities at the first-order phase transition, where clusters of high density form. In contrast to that, for an evolution through the critical point, the spherical structure from the initial conditions remains preserved, the system expands homogeneously.

One can translate these images into azimuthal distributions of the net-baryon number density as shown in Fig. 3. Here, the distributions are taken after $t = 6$ fm and $t = 12$ fm. They differ significantly for the different phase transition scenarios. For a crossover transition the curve is rather flat. When we increase the baryochemical potential we find small fluctuations starting around trajectories close to the critical point. Due to the present nonequilibrium effects we find strong fluctuations in the azimuthal distribution of net-baryon density for an evolution through the first-order phase transition. The bumps and deeps in the two plots are correlated, indicating that the clusters preserve their identity during the expansion. In experiment, these non-statistical fluctuations within single events should lead to an enhancement of higher flow harmonics. For the investigation this possibility a freeze-out scenario needs to be included, which gives the momentum distributions of e. g. net protons as a probe of net-baryon number. For further more quantitative results the use of

(a)

(b)

Figure 2: Relative net-baryon number density at $z = 0$ and $t = 9$ fm for (a) a first-order transition at and (a) for a transition through the critical point. Droplets of high density are formed at the first-order phase transition, at the critical point the density evolves homogeneously.

a more realistic model in terms of the low-energy phenomenology at high baryonic densities, like e. g. in [36], would be needed.

References

[1] Y. Aoki, G. Endrodi, Z. Fodor, S. D. Katz and K. K. Szabo, Nature **443** (2006) 675.

[2] S. Borsanyi *et al.* [Wuppertal-Budapest Collaboration], JHEP **1009** (2010) 073.

[3] W. Soldner [HotQCD Collaboration], PoS LATTICE **2010** (2010) 215.

[4] M. A. Stephanov, K. Rajagopal and E. V. Shuryak, Phys. Rev. Lett. **81** (1998) 4816
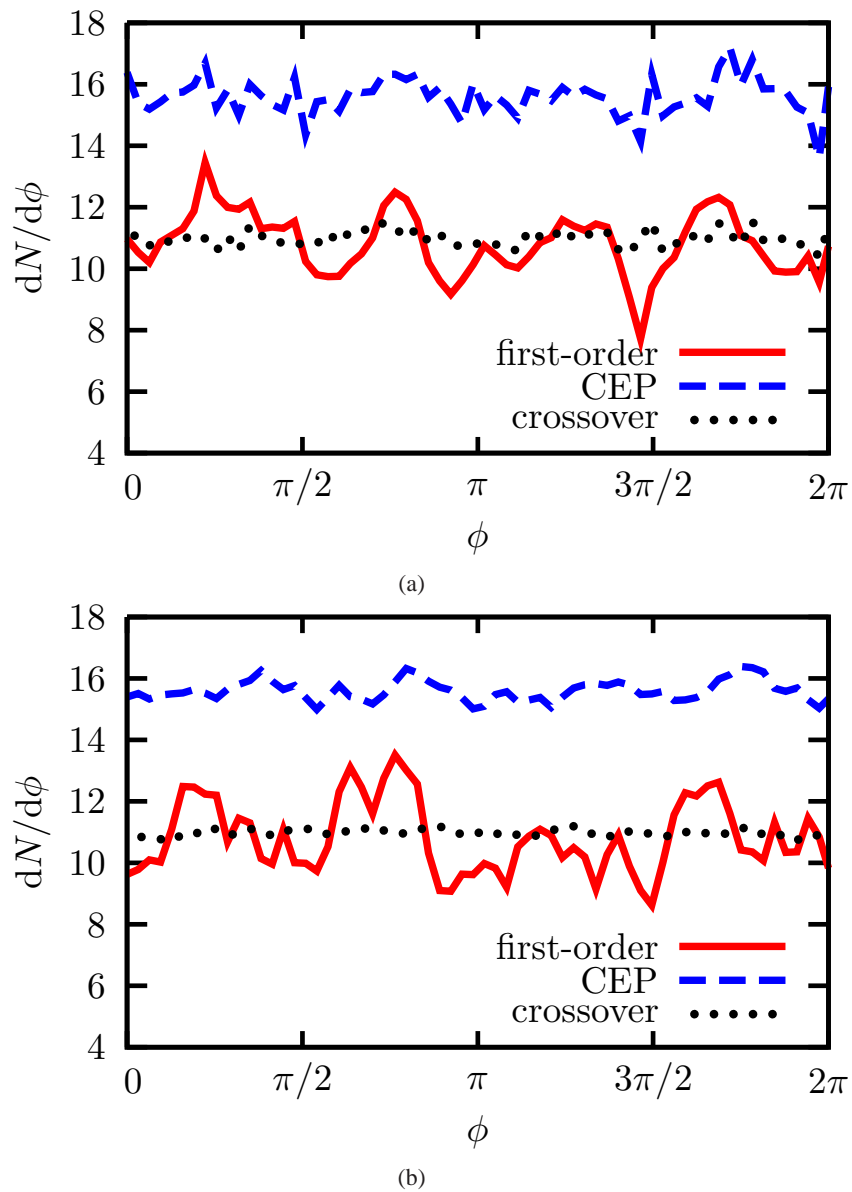
Figure 3: Azimuthal distribution of the net-baryon number density after $t = 6$ fm (a) and $t = 12$ fm (b) for several transition scenarios. Strong inhomogeneities develop at the first-order phase transition.

[5] M. A. Stephanov, K. Rajagopal and E. V. Shuryak, Phys. Rev. D **60** (1999) 114028.

[6] M. A. Stephanov, Phys. Rev. Lett. **102** (2009) 032301.

[7] O. Scavenius, A. Mocsy, I. N. Mishustin and D. H. Rischke, Phys. Rev. C **64** (2001) 045202.

[8] K. Fukushima, Phys. Lett. B **591** (2004) 277.

[9] B. -J. Schaefer and J. Wambach, Nucl. Phys. **A757** (2005) 479

[10] C. Ratti, M. A. Thaler, W. Weise, Phys. Rev. D **73** (2006) 014019.

[11] B. -J. Schaefer, J. M. Pawlowski, J. Wambach, Phys. Rev. D **76** (2007) 074023.

[12] V. Skokov, B. Friman and K. Redlich, Phys. Rev. C **83** (2011) 054904

[13] V. Skokov, B. Friman, E. Nakano, K. Redlich and B. -J. Schaefer, Phys. Rev. D **82** (2010) 034029

[14] B. -J. Schaefer, M. Wagner and J. Wambach, Phys. Rev. D **81** (2010) 074013

[15] C. Sasaki and I. Mishustin, Phys. Rev. C **85** (2012) 025202

[16] C. Sasaki, B. Friman and K. Redlich, Phys. Rev. D **77** (2008) 034024

[17] B. Berdnikov and K. Rajagopal, Phys. Rev. D **61** (2000) 105017.

[18] L. P. Csernai, J. I. Kapusta, Phys. Rev. D **46** (1992) 1379-1390.

[19] L. P. Csernai and I. N. Mishustin, Phys. Rev. Lett. **74** (1995) 5005.

[20] I. N. Mishustin, Phys. Rev. Lett. **82** (1999) 4779.

[21] O. Scavenius, A. Dumitru, E. S. Fraga, J. T. Lenaghan and A. D. Jackson, Phys. Rev. D **63** (2001) 116003

[22] J. Randrup, Phys. Rev. C **82** (2010) 034902.

[23] J. Steinheimer and J. Randrup, Phys. Rev. Lett. **109** (2012) 212301

[24] P. Chomaz, M. Colonna, J. Randrup, Phys. Rept. **389** (2004) 263-440.

[25] B. Schenke, S. Jeon and C. Gale, Phys. Rev. C **85** (2012) 024901.

[26] H. Petersen, J. Steinheimer, G. Burau, M. Bleicher and H. Stocker, Phys. Rev. C **78** (2008) 044901.

[27] M. Nahrgang, S. Leupold, C. Herold and M. Bleicher, Phys. Rev. C **84** (2011) 024912.

[28] T. S. Biro and C. Greiner, Phys. Rev. Lett. **79** (1997) 3138

[29] D. H. Rischke, Phys. Rev. C **58** (1998) 2331

[30] M. Nahrgang, S. Leupold and M. Bleicher, Phys. Lett. B **711** (2012) 109.

[31] M. Nahrgang, C. Herold, S. Leupold, I. Mishustin and M. Bleicher, J. Phys. G **40** (2013) 055108.

[32] C. Herold, M. Nahrgang, I. Mishustin and M. Bleicher, Phys. Rev. C **87** (2013) 014907.

[33] J. I. Kapusta, B. Muller and M. Stephanov, Phys. Rev. C **85** (2012) 054906

[34] C. Herold, M. Nahrgang, I. Mishustin and M. Bleicher, arXiv:1304.5372 [nucl-th].

[35] T. Kahara and K. Tuominen, Phys. Rev. D **78** (2008) 034015.

[36] J. Steinheimer, V. Dexheimer, H. Petersen, M. Bleicher, S. Schramm and H. Stoecker, Phys. Rev. C **81** (2010) 044913.